# The effect of medium refractive index on microparticle characterization by optical scattering

Sinan Genc*

*Faculty of Arts and Sciences, Middle East Technical University, Ankara 06800, Turkey*

Received October 04, 2024; accepted June 19, 2024; published June 30, 2024

**Abstract**—Considering microplastic pollution and the rapid accumulation of pollutants in the environment, it is necessary to have detailed information about the particles to describe their origin and take precautions. However, taking clear measurements and analyzing them can be challenging regarding the environment. In this study, input parameters of optical scattering, particle size and material, excitation laser, and refractive index of the medium and their effects are investigated. The effect of the medium is presented as Mie resonances for red, green, and blue lights. Machine learning results show that angle differences can be used for particle characterization in different environments.

Microplastic pollution has increased gradually over the last decade. Having particles in different environments, i.e., water resources, marine life, the placenta of mothers, newborn babies, and farm animals, proves that it is inevitable to be exposed to those contaminants once they have accumulated [1,2]. Therefore, precautions should be taken at the primary source of those pollutants. This would be possible if the particles were identified and characterized to determine the origin. Optical scattering allows for the detection and characterization of these contaminants by using their size, refractive index, and concentration. Studies in the literature aim to provide information about the samples by using small, cost-effective, and fast-response devices and setups [3,4]. Most of those devices analyze samples in water. However, the investigation of microplastics in different environments, i.e., human blood, oil, or others with different refractive indices, is also needed. In this study, the effect of the medium refractive index on light scattering will be investigated by using machine learning integrated numerical solutions. As there may be other particles in these environments, there may be a need for previous steps to gather microplastics in samples from nature. Although the equations of Mie theory work for the light scattering of single particles only, our previous study showed that it also applies to samples in water with 0.05 to 3.00 fM concentrations. Theoretical bright interference ring angles match with experimental values. Therefore, a code including Mie equations is used in this study to create a dataset for machine learning integration. Using different refractive indices of medium values, the performance of the machine learning algorithm is compared. The derivation of Mie solutions is given in the literature [5,6]. In the concept, the solution starts with the definition of the system geometry. The size and refractive index of the particle and wavelength of incident light are defined. Then, the size parameter dependent on particle radius and incident light is calculated. A plane wave with known frequency and polarization is defined as incident light. It impinges upon the particles and scatters. Conservation of electrical and magnetic fields needs appropriate boundary conditions to be applied. Scattering coefficients are calculated by Ricatti-Bessel functions, and finally, angular intensity functions are obtained as presented in Eqs. (1-2):

$$S_1(\theta) = \sum_{n=1}^{\infty} \frac{2n+1}{n(n+1)} \{a_n \pi_n(cos\theta) + b_n \tau_n(cos\theta)\} \quad (1)$$

$$S_2(\theta) = \sum_{n=1}^{\infty} \frac{2n+1}{n(n+1)} \{b_n \pi_n(cos\theta) + a_n \tau_n(cos\theta)\} \quad (2)$$

where $\pi_n$ and $\tau_n$ are Legendre polynomials and, $a_n$ and $b_n$ are scattering coefficients. Differential scattering cross sections are defined as presented in Eqs. (3-4):

$$\sigma'_{VV} = \frac{\lambda^2}{4\pi^2} |S_1(\theta)|^2 \quad (3)$$

$$\sigma'_{HH} = \frac{\lambda^2}{4\pi^2} |S_2(\theta)|^2 \quad (4)$$

where $\lambda$ is the wavelength of the incident light, subscription VV refers to vertically polarized incident light and vertically polarized scattered light, and HH refers to the horizontally polarized incident and scattered light. The other versions, *VH* and *HV*, have too small contributions, which are ignored. The code written in MATLAB is given in [7], and the match between theoretical calculations and experimental results was shown in our previous works [8,9]. Nested for-loops are used to have data for each combination of input parameters. 3 to 7 μm for particle size (d) with 0.5 μm increments, 1.3 to 2 with 0.01 increments for particle refractive index ($n_{part}$) and three different wavelengths are used. 650 nm, 520 nm, and 440 nm are decided for red, green, and blue lasers, respectively. For the key point of this study, medium refractive index ($n_{med}$),

* E-mail: sgenc@metu.edu.tr

 

1.2 to 1.7 with 0.01 increments is used as the range targeted. This range includes water, milk, human blood, alcohol, oils, and xylene as high-refractive-index solvents. As expected, numerical solutions showed that when increasing the particle size results in more dominant forward scattering when the other input parameters are kept constant. At the same time, Mie resonances near the zero-degree get closer to each other, and more peaks are observed compared to larger particles at the same angle range. While one wide peak occurs for 4.5 μm particles for red light in Fig.1(a), there are three peaks for 6.5 μm particles. In addition, for each input laser, the highest intensity occurs at the biggest particle at the lowest degree, which proves the dominant forward scattering. Furthermore, at the same color scale, the highest intensity of red has a lower value than the highest intensity value of blue, showing that at shorter wavelengths of input light, forward scattering is more dominant than the ones at longer wavelengths. Therefore, it can be clearly said that the bigger the particle, the stronger the forward scattering, and the greater number of peak angles.

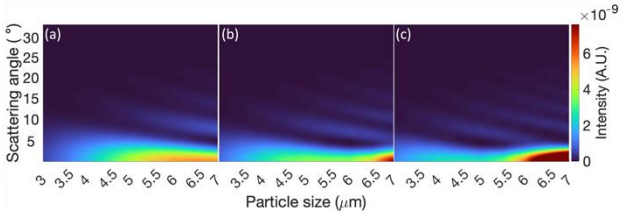


Fig. 1. Change of scattering intensity by particle size for (a) 650 nm, (b) 520 nm, and (c) 440 nm laser by Mie theory for $n_{part}$=1.4 and $n_{med}$=1.3.

About another input parameter, the refractive index of the particle, at the same medium, it is expected to have more scattered light at wider angles, which provides a smaller number of peaks at the same angle range, as given in Fig. 2, when the refractive index of the particle is higher. As in Fig.2(b), when the refractive index of the particle is increased, the difference between the refractive indices of the medium and the particle gets increased. Therefore, light scatters more, and forward scattering gets weaker. In addition, among three different input wavelengths, the shortest wavelength results in the highest forward scattering intensity compared to other wavelengths.

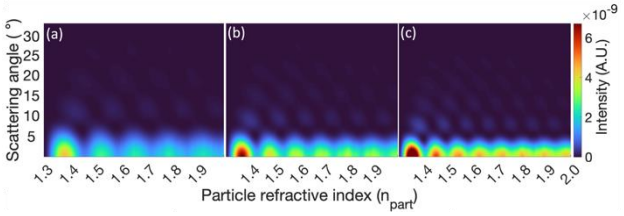


Fig. 2. Change of scattering intensity by $n_{part}$ for (a) 650 nm, (b) 520 nm, and (c) 440 nm laser by Mie theory for d=5 $\mu$m and $n_{med}$=1.3.

The last input parameter, the refractive index of the medium, is one of the key factors to detect and define the particles. As presented in Fig. 3, increasing the value of the medium refractive index, as in the investigation of the particle refractive index, decreases the scattered light intensity at Mie resonances. While the highest level of forward scattering is observed at the near-zero difference between refractive indices of the medium and the particle, as clear and expected, no scattering occurs when those values are equal to 1.4.

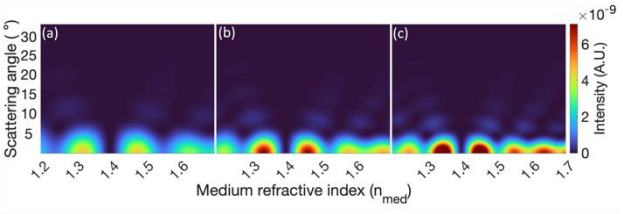


Fig. 3. Change of scattering intensity by $n_{med}$ for (a) 650 nm, (b) 520 nm, and (c) 440 nm laser by Mie theory for $d$=5 μm and $n_{part}$=1.4.

The evaluation of the scattering data of a sample at known wavelengths of incident light and interference ring angles is critical regarding the background refractive index. Therefore, the characterization of the same samples in different environments provides an opportunity to have information about the effect of the refractive index of the environment. To visualize the effect of different environments with different refractive indices, i.e., water, blood, glycerol, and o-xylene, silicon dioxide, nylon 6, polystyrene (PS), and polyethylene terephthalate (PET) have been chosen as particles in those environments, as presented in Table 1.

Table 1. Refractive indices of the medium and the particles for red, green, and blue lights.

| | **650 nm** | **520 nm** | **440 nm** |
|---|---|---|---|
| Water [10] | 1.331 | 1.334 | 1.337 |
| Blood [11] | 1.346 | 1.350 | 1.355 |
| Glycerol [12] | 1.470 | 1.475 | 1.479 |
| o-Xylene [13] | 1.499 | 1.512 | 1.524 |
| Silicon dioxide [14] | 1.46 | 1.46 | 1.47 |
| Nylon 6 [15–17] | 1.53 | 1.53 | 1.53 |
| PS [18] | 1.59 | 1.60 | 1.62 |
| PET [19] | 1.56 | 1.58 | 1.60 |

Mie resonances and bright interference ring angles for each environment are given in Fig. 4 on normalized scattering distributions. As the triangles show the peak points, even a 0.03 difference in the refractive indices of the particles moves the peaks on the *x*-axis. Thus, machine learning tools can be used to distinguish those particles in different environments for fast and accurate characterization. Random Forest is an easy-to-use algorithm that provides consistent results for these types of applications, as given in the literature [20,21].

The same input parameter ranges as in theoretical calculations of Mie theory, 1.2 to 1.7 for $n_{med}$, 1.3 to 2 for $n_{part}$, and 650 nm, 520 nm, 440 nm for red, green, and blue

 

lasers were used to create a dataset for Random Forest algorithm. A particle size of 5 μm was used as a constant parameter for controlled refractive index analysis.

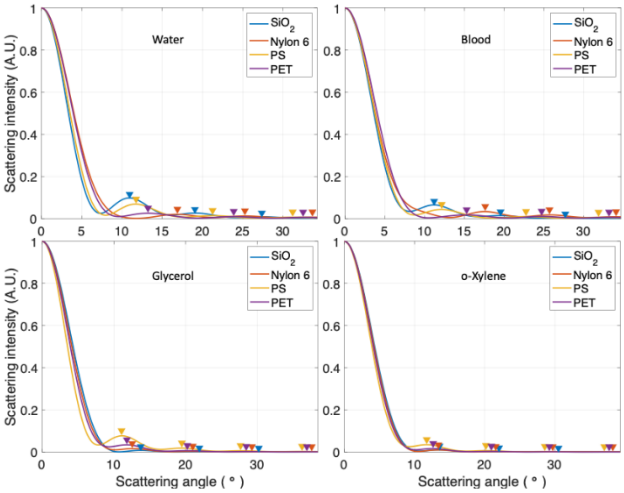


Fig. 4. Mie resonances of four particles in (a) water, (b) blood, (c) glycerol, and (d) o-Xylene at 650 nm laser.

Calculated first four peak angles were added to this dataset. Then, to train the Random Forest model, 90% (7860 lines) of the peak angles and wavelength of the light source were given as input parameters, and the remaining part, 10% (873 lines), was used as test data. The refractive index of the particle was aimed at being predicted. The average error between predicted and actual values of particle refractive indices of 873 lines was 0.0023. To evaluate the appropriateness of conducting independent variable t-tests, it is imperative that the data distribution adheres to a normal pattern. The analysis reveals that the skewness and kurtosis values of the actual data are -0.006 and -1.228, respectively, which are deemed to be within an acceptable range. Likewise, the skewness and kurtosis values of the test data, specifically 0.002 and -1.242 respectively, fall within the allowed range for conducting independent sample t-tests. The obtained significance value (0.624) from Levene's test for equal variances indicates that the assumption of equal variances is satisfied for the dataset under consideration. Under the assumption of equal variances between the actual ($\bar{x}$=1.5022) and predicted data ($\bar{x}$=1.4999), the findings of the independent sample t-test, conducted with a 95% confidence interval, indicate that there is no statistically significant distinction between the mean values of the actual and predicted data. The t-statistic is calculated to be 0.409, with degrees of freedom (df) equal to 1744. Furthermore, the obtained two-sided p-value (0.682) exceeds the threshold of 0.05.

In summary, it is feasible to employ machine learning techniques to address the inverse light scattering theory, thereby enabling the determination of the refractive index of a 5 μm spherical particle within media exhibiting varying refractive indices. Despite minor variations in Mie resonances, machine learning consistently yields accurate predictions. However, as microplastics are not ideally spherical and mono-dispersed in nature, there may needs to have previous steps i.e., filtering, centrifuge before using this low-cost setup. The scope of the inquiry can be expanded to include further applications pertaining to particle size, encompassing not only microplastics but also several other particle types.

## References

[1] Q. Zhang, E.G. Xu, J. Li, Q. Chen, L. Ma, E.Y. Zeng, H. Shi, Environ. Sci. Technol. **54**, 3740 (2020).
[2] L.M. Hernandez, E.G. Xu, H.C.E. Larsson, R. Tahara, V.B. Maisuria, N. Tufenkji, Environ. Sci. Technol. **53**, 12300 (2019).
[3] C.K. Chen, J. Zhang, A. Bhingarde, T. Matotek, J. Barrett, B.D. Hardesty, M.M. Banaszak Holl, B.L. Khoo, Chem. Eng. J. **428**, 132614 (2022).
[4] A.H. Iri, M.H.A. Shahrah, A.M. Ali, S.A. Qadri, T. Erdem, I.T. Ozdur, K. Icoz, Env. Science and Pollution Research **28**, 63860 (2021).
[5] C.F. Bohren, D. R. Huffman, *Absorption and scattering of light by small particles* (New York, Wiley, 1983).
[6] H.C. van de Hulst, *Light scattering by small particles* (New York, Dover Publications, 1981).
[7] "sinanngenc/miemtlb: Mie scattering calculations by MATLAB," https://github.com/sinanngenc/miemtlb (March 20, 2024).
[8] S. Genc, K. Icoz, T. Erdem, R. Soc. Open Sci. **10**, 230586 (2023).
[9] S. Genc, T. Erdem, K. Icoz, Sensors and Actuators: A. **370**, 115265 (2024).
[10] Refractive index of $H_2O$, $D_2O$ (Water, heavy water, ice)" https://refractiveindex.info/?shelf=main&book=H2O&page=Hale (March 20, 2024).
[11] S. Liu, Z. Deng, J. Li, J. Wang, N. Huang, R. Cui, Q. Zhang, J. Mei, W. Zhou, C. Zhang, Q. Ye, J. Tian, J. Biomed. Opt. **24**, 1 (2019).
[12] "Refractive index of $C_3H_5(OH)_3$ (Glycerol)" https://refractiveindex.info/?shelf=organic&book=glycerol&page=Birkhoff (March 20, 2024).
[13] J.E.F. Rubio, J.M. Arsuaga, M. Taravillo, V.G. Baonza, M. Cáceres, Exp. Therm. Fluid Sci. **28**, 887 (2004).
[14] "Refractive index of $SiO_2$ (Silicon dioxide, Silica, Quartz)" https://refractiveindex.info/?shelf=main&book=SiO2&page=Malitson (March 20, 2024).
[15] "Physical properties of plastics" https://www.professionalplastics.com/professionalplastics/content/downloads/PhysicalPropertiesofPlastics.pdf (March 20, 2024).
[16] "Refractive Index of Polymers by Index" https://scipoly.com/technical-library/refractive-index-of-polymers-by-index/ (March 20, 2024).
[17] H.A. Gaur, H. De Vries, J. Polymer Science: Polymer Phys. Edition **13**, 835 (1975).
[18] "Refractive index of $(C_8H_8)_n$ (Polystyrene)" https://refractiveindex.info/?shelf=organic&book=polystyren&page=Sultanova (March 20, 2024).
[19] "Refractive index of $(C_{10}H_8O_4)_n$ (Polyethylene terephthalate)" https://refractiveindex.info/?shelf=organic&book=polyethylene_terephthalate&page=Zhang (March 20, 2024).
[20] M.Z. Joharestani, C. Cao, X. Ni, B. Bashir, S. Talebiesfandarani, Atmosphere, **10**, 373 (2019).
[21] J.L. Speiser, M.E. Miller, J. Tooze, E. Ip, Expert Syst. Appl. **134**, 93 (2019).

 